Influence of the tip clearance on the auto-oscillation frequency of a cavitating pump

IOP Conf. Series: Earth and Environmental Science **240** (2019) 032050 doi:10.1088/1755-1315/240/3/032050

Influence of the tip clearance on the auto-oscillation frequency of a cavitating pump

Peter F. Pelz[1], **Paul Taubert**[2]

Chair of Fluid Systems, Technische Universität Darmstadt, Otto-Berndt-Str. 2, 64287 Darmstadt, Germany.

[1] Professor and Head of Chair

[2] Research Assistant

E-mail: peter.pelz@fst.tu-darmstadt.de

Abstract. This paper gives a contribution to the vortex structure, vortex dynamics and the tip clearance inertance as well as compliance of a cavitating pump. The related vortex structure is reduced to the blade bound vortices, hub vortex and tip vortices only. At heavy part load $\varphi \to 0$, the tip vortices form a coaxial vortex ring of increasing strength. This vortex ring may break down to several wall bound vortices at severe part load. The velocity potential of the vortex ring is given by the Bessel series solution and by applying a limit value analysis. The inertance of the gap flow is derived straight forward from this generic mathematical model of an axial pump at deep part load. With the compliance due to cavitation, the natural frequency of cavitation surge is discussed for the given generic mathematical model of the pump.

1. Introduction

The task of this paper is the determination of analytic expressions for the inertance L and compliance C of the tip clearance flow of an axial pump. The work extends the research of Brennen, 2016 [1] employing a recently developed vortex model of an axial turbomachine at part load (cf. Pelz & Taubert, 2017 [2]). This model is recapped in the following. Figure 1a shows the vortex model of the pump. The N bound vortices of strength Γ form the hub vortex of strength $N\Gamma$ and the tip vortices. At part load $\varphi = U/(\Omega R) \to 0$ (averaged velocity U, pipe radius R, rotational speed of the pump Ω), the tip vortices feed a coaxial vortex ring, whose radius equals the tip radius R_t. The strength Γ_t of this vortex ring is increasing in time until a critical value is reached. It is suspected that this might reason a self-excited process like the periodic cavity cloud separation (cf. Pelz & Taubert, 2017 [2]).

Figure 1b shows the streamlines derived from this model in the meridian plane for the ratio $\beta := R_t/R = 0.8$ and a vortex strength of the ring vortex Γ_t of $\Gamma_t = 10\,U R_t$.

The vortex model is a coarse geometric model of the real flow which may serve gaining insights into the dynamics of a cavitating pump extending the work of Brennen.

Figure 2b shows the lumped parameter model of the same pump. Brennen [1, 3] proposed a more detailed model taking a main flow and a by-pass flow into account. Nevertheless, there are indications that the tip clearance mainly influences the pressure build up and not so much the internal leakage of the flow (cf. Karstadt & Pelz, 2012 [4]). This behaviour is different to radial pumps where the internal leakage shall not be neglected. With respect to the inertance of the flow, one has to keep in mind that most of the integral kinetic energy of the flow is due to

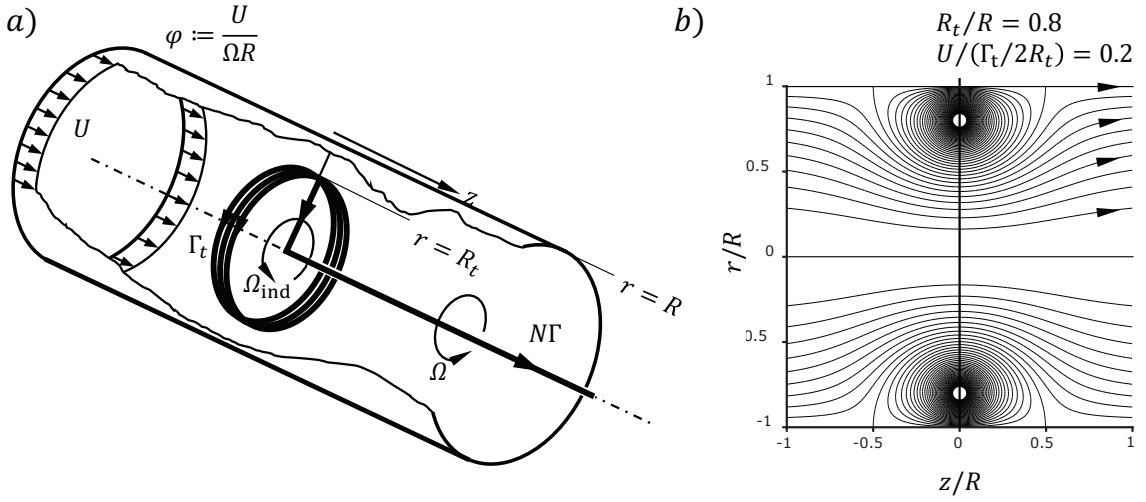

Figure 1. a) generic vortex system of an axial pump at part load; b) streamlines in the meridian plane (cf. Pelz & Taubert, 2017 [2]).

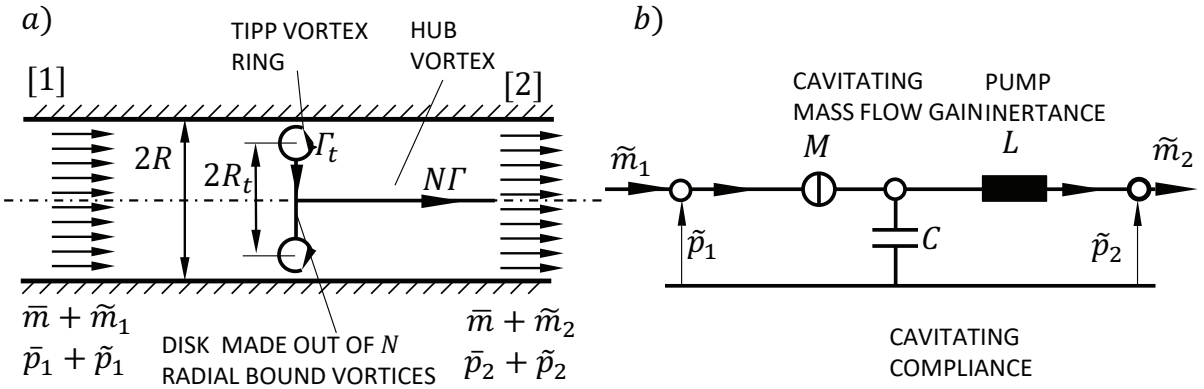

Figure 2. a) Vortex model of an axial pump at part load [2]; b) lumped parameter model of an axial pump.

the tip vortex flow. This is mainly because the tip vortex is located at a large radius $R_t \to R$. Hence, it is sufficient in a first approach to concentrate on the inertance of the tip vortex flow. Indeed, this is the focus and novelty of this paper.

2. Linear perturbation expansion and dimensional analysis

Taking disturbances up to the first order into account, the usual perturbation approach is done: the pressure on the suction and pressure side are expanded as $p_1(t) = \bar{p}_1 + \tilde{p}_1(t)$, $p_2(t) = \bar{p}_2 + \tilde{p}_2(t)$. Similar the mass flow rate on both sides of the pump are perturbed: $m_1(t) = \bar{m} + \tilde{m}_1(t)$, $m_2(t) = \bar{m} + \tilde{m}_2(t)$. Considering only linear terms in the expansion, the transform such as $\tilde{m} = \Re\left[\hat{m}_1 \exp\left(\mathrm{i}\omega t\right)\right]$ is made for all fluctuating quantities. The remaining equation for perturbations to the power zero is the pump characteristic

$$\bar{p}_2 - \bar{p}_1 = \Delta p(\bar{m}). \tag{1}$$

The remaining equation for the linear perturbation is the transfer characteristics given by the relation

$$\begin{bmatrix} P_{11} & P_{12} \\ P_{22} & P_{21} \end{bmatrix} \begin{bmatrix} \hat{p}_1 \\ \hat{m}_1 \end{bmatrix} = \begin{bmatrix} \hat{p}_2 \\ \hat{m}_2 \end{bmatrix}. \tag{2}$$

The momentum and continuity equation solve the elements P_{ij} of the dynamic transfer characteristics. The momentum equation in three equivalent representations yields:

$$\varrho l \pi R^2 \dot{U}_2 = \dot{\tilde{m}}_2 l = \dot{I} = \pi R^2 (\tilde{p}_1 - \tilde{p}_2). \tag{3}$$

U_2 is the area averaged velocity at the outlet, l is the inductive length and $\dot{I}$ the rate of change of the axial momentum. With the inductive length l of the pump being determined as it will be done in the following section, the inertance L of the pump is given by $Ll/\pi R^2$. As an orientation, the inductive length of a simple aperture in an unlimited plane wall of infinite thickness is $R_t \approx \pi/4 R_t$ [5]. For the low pressure LOX inducer in the Space Shuttle main engine, Brennen derives the approximation $L \approx 10/R_t$ from measurements, i.e. the inductive length of this inducer is nearly thirty times the tip radius: $l = L\pi R^2 \approx 30 R_t$. The continuity equation, ignoring cavitating mass flow gain, reads

$$\frac{\varrho V_\varepsilon}{n \bar{p}_1} \dot{\tilde{p}}_1 - \tilde{m}_1 + \tilde{m}_2 = 0, \tag{4}$$

where V_ε is the cavity volume. This investigation ingnores the mass flow gain due to cavitation as it mainly influences the damping and not the frequency itself. In the following, the abbreviation for the hydraulic compliance $C := \varrho V_\varepsilon/(n\bar{p}_1)$ is used. The polytropic exponent n equals one for a "small" cavity and equals $\gamma = 1.4$ for a "large" cavity [6]. With the abbreviations L and C and the transformation into the frequency domain, we derive

$$\left(1 + \omega^2 LC\right) \hat{p}_1 - \mathrm{i}\omega L \hat{m}_1 = \hat{p}_2, \tag{5}$$

$$-\mathrm{i}\omega C \hat{p}_1 + \hat{m}_1 = \hat{m}_2. \tag{6}$$

The pressure shall be non-dimensionalyzed by the dynamic pressure $\varrho\Omega^2 R_t^2$ and the mass flow rate by $\varrho\Omega R_t^3$. Dividing the first equation by $\varrho\Omega^2 R_t^2$ and the second equation by $\varrho\Omega R_t^3$ we obtain

$$\left(1 + \omega_+^2 L_+ C_+\right) \hat{p}_{1+} - \mathrm{i}\omega_+ L_+ \hat{m}_{1+} = \hat{p}_{2+}, \tag{7}$$

$$-\mathrm{i}\omega_+ C_+ \hat{p}_{1+} + \hat{m}_{1+} = \hat{m}_{2+}. \tag{8}$$

By inspection we gain the dimensionless products to be

$$\omega_+ := \frac{\omega}{\Omega}, \quad L_+ := L R_t = \frac{l\beta^2}{\pi R_t}, \quad C_+ := \frac{C\Omega^2}{R_t} = \frac{1}{n}\frac{V_\varepsilon}{R_t^3}\frac{\varrho\Omega^2 R_t^2}{\bar{p}_1} \approx \frac{2}{n}\frac{V_\varepsilon}{R_t^3}\frac{1}{\sigma} \text{ for } \bar{p}_1 \gg p_\mathrm{v}. \tag{9}$$

Hence, the pump compliance is inverse proportional to the cavitation number $\sigma := 2(\bar{p}_1 - p_\mathrm{v})/(\varrho\Omega^2 R_t^2)$, assuming the vapour pressure is much smaller than the suction pressure: $p_1 \gg p_\mathrm{v}$. This result is not new, but the dimensional analysis is indeed a nice affirmation. We now employ the vortex model sketched in Figure 1 and 2: we assume the cavity volume V_ε to be the core of the coaxial vortex ring shown in Figure 1. If the core radius is $\delta = \varepsilon R_t/2$, the volume is given by $V_\varepsilon = \pi^2 R_t^3 \varepsilon^2/4$. With this the dimensionless compliance yields

$$C_+ = \frac{(\pi\varepsilon)^2}{2n}\frac{1}{\sigma}. \tag{10}$$

From the mentioned performance experiments of the low pressure LOX inducer in the Space Shuttle main engine, Brennen derived the approximation $C_+ \approx 0.05\,\sigma^{-1}$. Comparing this datum with the result from equation (10) we estimate $\varepsilon \approx 0.1 \ldots 0.12$ for $1 \le n \le \gamma = 1.4$. Thus, the core radius δ of the ring vortex ring is estimated to be

$$\delta \approx (0.05 \ldots 0.06)\, R_t. \tag{11}$$

3. Inertance of the pump derived from the velocity potential

In the coarse-graining limit model, the core of the vortex ring is seen as a washer-like vortex sheet located at $z = 0$, $R_t(1-\varepsilon) < r < R_t$. The tangential to the surface of the sheet is W at $z = 0_+$ and $-W$ at $z = 0_-$. Hence, the circulation of the vortex ring is $\Gamma_t = 2\varepsilon R_t W$. Alternatively the strength of the vortex ring is given by the dimensionless product

$$\tau := \frac{\Gamma_t}{2R_t U} = \varepsilon \frac{W}{U}. \tag{12}$$

From Euler's equation and the energy equation we derive the pump characteristics $N\Gamma\Omega/2\pi = (\Omega R_t)^2(1-\varphi/\hat{\varphi})$ and thus $N\Gamma\Omega/2\pi \to (\Omega R_t)^2$ for $\varphi \to 0$ [2]. In our model, the N tip vortices of strength Γ roll up in time t to form $\Gamma_t = N\Gamma\Omega t/2\pi$ [2]. With the ratio $\beta := R_t/R = 1-s$, where s is the dimensionless tip clearance, there is an upper bound for τ. The pump performance affects the upper bound to be $\Gamma_t < (\Omega R_t)^2 t$ at severe part load $\varphi \to 0$, yielding

$$\tau := \frac{\Gamma_t}{2R_t U} = \frac{1}{2}\frac{\Omega t}{2\pi}\frac{N\Gamma}{R_t U} < \frac{\Omega t}{2}\frac{\beta}{\varphi}. \tag{13}$$

The velocity potential ϕ_ε of the coaxial vortex ring in a parallel flow is

$$\frac{\phi_\varepsilon(r,z)}{UR} = \frac{z}{R} - 2\tau \sum_{n=1}^{\infty} \frac{1}{k_n J_0^2(k_n)} J_0\left(k_n \frac{r}{R}\right) \exp\left(-k_n \frac{|z|}{R}\right) \frac{1}{\varepsilon} \int_{\beta(1-\varepsilon)}^{\beta} J_1\left(k_n \frac{r}{R}\right) \frac{r}{R}\, \mathrm{d}\left(\frac{r}{R}\right), \tag{14}$$

as derived by Pelz & Taubert, 2017 [2]. The numbers k_n for $n = 1, ..., \infty$ are the roots of the Bessel function: $J_1(k_n) = 0$. For $\varepsilon W = \tau U = \text{const.}$ and $\varepsilon \to 0$ the integral simplifies to the expression

$$\lim_{\varepsilon \to 0} \frac{1}{\varepsilon} \int_{\beta(1-\varepsilon)}^{\beta} J_1\left(k_n \frac{r}{R}\right) \frac{r}{R}\, \mathrm{d}\left(\frac{r}{R}\right) = \beta^2,\, J_1(k_n \beta) \tag{15}$$

applying L'Hôpital's rule. Hence, we have the singular solution for the coaxial ring vortex in the tube with its flow potential

$$\frac{\phi_\varepsilon(r,z)}{UR} \to \frac{\phi(r,z)}{UR} = \frac{z}{R} - 2\tau\beta^2 \sum_{n=1}^{\infty} \frac{J_1(k_n\beta)}{k_n J_0^2(k_n)} J_0\left(k_n \frac{r}{R}\right) \exp\left(-k_n \frac{|z|}{R}\right). \tag{16}$$

The contour lines of the related Stokes stream function

$$\frac{\psi(r,z)}{UR} = -\frac{1}{2}\left(1 - \frac{r^2}{R^2}\right) + 2\tau\beta^2 \sum_{n=1}^{\infty} \frac{J_1(k_n\beta)}{k_n J_0^2(k_n)} J_1\left(k_n \frac{r}{R}\right) \frac{r}{R} \exp\left(-k_n \frac{|z|}{R}\right). \tag{17}$$

are plotted in Figure 1b. With the result of equation (14) we are now set to derive an analytic expression for the inertance L_+ of the pump. Following Saffmann [7], the momentum used in the momentum equation (3), $\dot{I} = A(\tilde{p}_1 - \tilde{p}_2)$, yields

$$\begin{aligned} I &= \varrho \int_{S_\mathrm{B}} \phi_\varepsilon\, \vec{n} \cdot \vec{e}_z\, \mathrm{d}S_\mathrm{B} = -4\pi R^2 \varrho \int_{\beta(1-\varepsilon)}^{\beta} \phi_\varepsilon(r, 0_+) \frac{r}{R}\, \mathrm{d}\left(\frac{r}{R}\right) \\ &\approx 8\pi R^3 U \tau \varrho \sum_{n=1}^{\infty} \frac{J_1(k_n\beta)\beta^2}{k_n J_0^2(k_n)} \int_{\beta(1-\varepsilon)}^{\beta} J_0\left(k_n \frac{r}{R}\right) \frac{r}{R}\, \mathrm{d}\left(\frac{r}{R}\right) \end{aligned} \tag{18}$$

for small $\varepsilon \to 0$. The hydrodynamic impulse of the bound vorticity equals the virtual momentum since the volume of the body is zero. The integral is approximated by

$$\int_{\beta(1-\varepsilon)}^{\beta} J_0\Big(k_n \frac{r}{R}\Big)\, \frac{r}{R}\, \mathrm{d}\Big(\frac{r}{R}\Big) \approx \varepsilon \beta^2 J_0(k_n \beta). \tag{19}$$

Hence, the momentum yields

$$I = 8 m R_t \varepsilon \tau \beta^3 \sum_{n=1}^{\infty} \frac{J_1(k_n\beta)\, J_0(k_n\beta)}{k_n J_0^2(k_n)}, \tag{20}$$

with the mass flux $m = \varrho U \pi R^2$. From equation (3) we obtain $\dot{\tilde{m}}_2 l = \dot{I}$ or with $l = L\pi R^2 = L_+ \pi R_t/\beta^2$ the reduced inertance of the pump

$$L_{\mathrm{red}}(\beta) := \frac{L_+}{\varepsilon\tau} = \frac{8\beta^5}{\pi} \sum_{n=1}^{\infty} \frac{J_1(k_n\beta)\, J_0(k_n\beta)}{k_n J_0^2(k_n)}. \tag{21}$$

The reduced inertance of the pump is plotted versus the dimensionless tip clearance $s = 1 - \beta$ in Figure 3 for $0 < s < 0.1$. For small tip clearance $s \to 0$ the reduced inertance tends to its maximal value and decreases with increasing tip clearance.

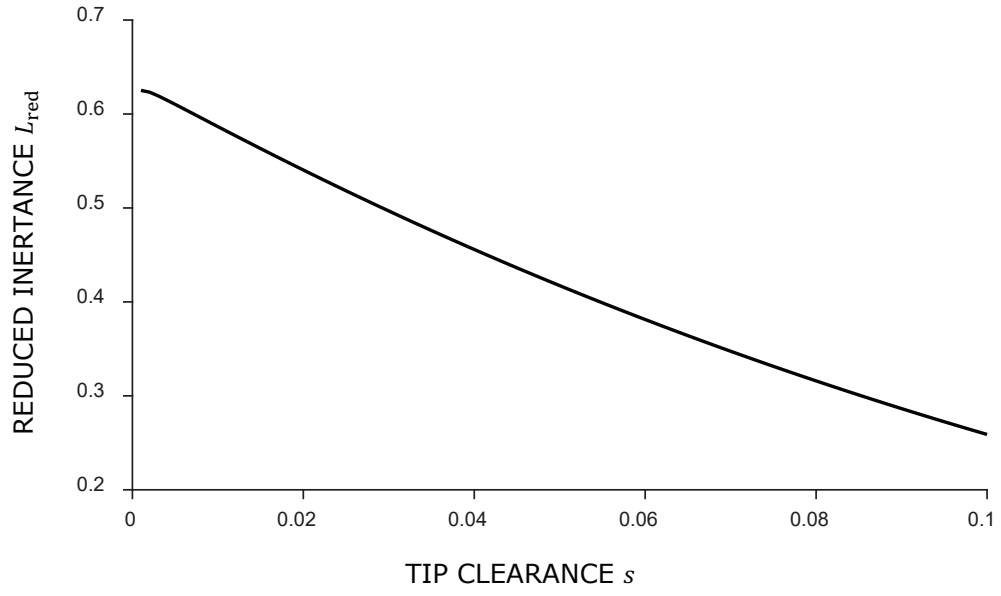

Figure 3. Reduced inertance L_{red} over tip clearance s, equation (21).

From result (21), the auto-oscillation frequency of the pump is determined to be

$$\frac{\omega_A}{\Omega} = (C_+ L_+)^{-1/2} = \left(\frac{1}{\pi^2} \frac{2n}{L_{\mathrm{red}}(s)} \frac{\sigma}{\tau \varepsilon^3} \right)^{1/2}. \tag{22}$$

With the results of Brennen, i.e. $\omega_A/\Omega = (2\sigma)^{1/2},\ n \approx 1,\ \varepsilon \approx 0.1$ the typical dimensionless circulation is of the order

$$\tau(s) \approx \frac{1000}{\pi^2}\frac{1}{L_{\mathrm{red}}(s)} \approx \frac{100}{L_{\mathrm{red}}(s)}. \tag{23}$$

The upper bound, equation (12), is due to the pump characteristics with the flow number $\varphi = U/\,R\Omega$.

4. Conclusion

The results derived within the framework of this paper highlight that an analytical approach leads to the determination of both, inertance L and compliance C of the tip clearance flow of an axial pump. For this case the influence of the tip vortex on the pressure build up is higher than the internal leakage of the flow (cf. Karstadt & Pelz, 2012 [4]). Hence, these characteristics are of great importance for calculating the transfer behavior of these types of turbomachines. With this in mind, the investigation derives the auto-oscillation frequency of an axial pump.

References

[1] C E Brennen. On the Dynamics of a Cavitating Pump. *IOP Conference Series: Earth and Environmental Science*, 49:052018, 2016.
[2] P F Pelz, P Taubert, and F-J Cloos. Vortex Structure and Kinematics of Encased Axial Turbomachines. In *17th International Symposium on Transport Phenomena and Dynamics of Rotating Machinery*, Maui, Hawaii, USA, 2017.
[3] C E Brennen. Bubbly flow model for the dynamic characteristics of cavitating pumps. *Journal of Fluid Mechanics*, 89(2):223–240, 1978.
[4] S Karstadt and P F Pelz. A Physical Model for the Tip Vortex Loss: Experimental Validation and Scaling Method. In *ASME Turbo Expo 2012: Turbine Technical Conference and Exposition*, pages 73–81, Copenhagen, Denmark, 2012. American Society of Mechanical Engineers.
[5] J W S Rayleigh. *The Theory of Sound*, volume 2. New York, 1945.
[6] P F Pelz and J Buttenbender. The dynamic stiffness of an air-spring. In *International Conference on Noise & Vibration Engineering ISMA*, Leuven, Belgium, 2004.
[7] P G Saffman. *Vortex Dynamics*. Cambridge University Press, 1992.